

LHC diphoton excess from colorful resonancesJia Liu ^{1,*}, Xiao-Ping Wang ^{1,†} and Wei Xue ^{2‡}¹*PRISMA Cluster of Excellence and Mainz Institute for Theoretical Physics,
Johannes Gutenberg University, 55099 Mainz, Germany*²*Center for Theoretical Physics, Massachusetts Institute of Technology, Cambridge, MA 02139, USA*

(Dated: March 10, 2022)

Motivated by the possible diphoton excess around 750 GeV observed by ATLAS and CMS at 13 TeV, we consider a coloron model from $SU(3)_1 \times SU(3)_2$ spontaneously breaking to the Standard Model $SU(3)_C$. A colored massive vector boson is resonantly produced by $q\bar{q}$ in proton collision, followed by a colored scalar cascade decay. This process gives two photons and one jet in the final states. And the kinetic edge of the two photons can be an interpretation of the diphoton excess, while satisfying the dijet, $t\bar{t}$, jet+photon resonance constraints. In this model, due to the large mass of vector resonance, the parton luminosity function ratio between 13 TeV and 8 TeV can be quite large. Therefore, the diphoton excess has not been observed at 8 TeV search. On the other hand, having all the new particles color-charged around TeV, this model predicts new signals at the LHC, which can be validated soon.

* Email: liuj@uni-mainz.de

† Email: xiaowang@uni-mainz.de

‡ Email: weixue@mit.edu

CONTENTS

I. Introduction	2
II. Model	3
II.1. spontaneous breaking down to $SU(3)_C$	3
II.2. The interactions for extra fermions and scalars	4
II.3. The decay and production of G' and S	5
III. Constraints for the model	6
IV. Diphoton signal from cascade decay of G'	8
V. Summary and Conclusion	10
Acknowledgments	11
References	11

I. INTRODUCTION

ATLAS and CMS collaborations present their RUN 2 results on inclusive diphoton search [1, 2] at $\sqrt{s} = 13\text{TeV}$. Both of the experiments reveal an excess in the diphoton $m_{\gamma\gamma}$ spectrum near 750 GeV. Having 3.2 fb^{-1} data, ATLAS gives 3.9 (2.3) σ local (global) significance for broad resonance search and 3.6 (2.0) σ local (global) significance for narrow width approximation. CMS have 2.6 fb^{-1} data and gives 2.6 σ local significance. Although this excess could be statistical fluctuations, it motivates many new physics explanations [3–80].

Due to Laudaun-Yang theorem [81, 82], the excess can be explained by 750 GeV spin-0 particle produced resonantly, and meanwhile it needs other particles introduced to have the right coupling to proton proton and to photon photon. Most of the models interpret the excess by introducing a singlet scalar, while in our paper, we use particles with the Standard Model (SM) $SU(3)_C$ color charge to produce the diphoton resonance. We consider a coloron model, $SU(3)_1 \times SU(3)_2 \rightarrow SU(3)_C$ to give an alternative way to reproduce the excess in the diphoton spectrum. The cascade decay of heavier colored particle to lighter colored particle, can produce the kinetic edge in the diphoton invariant mass spectrum, see fig. 1. This model is consistent with the collider constraints, like dijet, $t\bar{t}$ and jet+ γ resonance at both 8 (13) TeV and also safe from diphoton resonance search at 8 TeV. The model also predicts unique event topology, different from the 750 GeV scalar resonance, including new resonances and different kinetic distribution of the final state particles.

The paper is organized as follows. In section II, we introduce the coloron model, where a heavy color particle is the massive gauge field after symmetry breaking and a relative lighter extra scalar is color charged as well. The cascade decay of the two particles produce two photons and one gluon in the final states, which generate a kinetic edge in the di-photon spectrum. In section III, we discuss the LHC constraints on the model from dijet, $t\bar{t}$, jet+ γ and diphoton resonance searches at 8 and 13 TeV. We find that the parameter space which can explain the di-photon excess can be consistent with those collider constraints. In section IV, we study the signal diphoton invariant mass spectrum and its other kinetic properties. We summarize our results in section V.

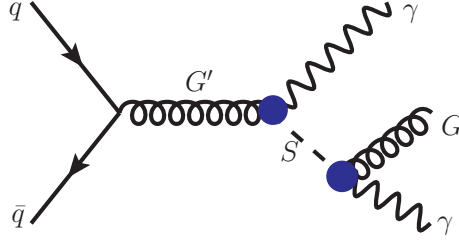


Figure 1. The Feynman diagram for resonance production of G' , which subsequently cascade decay to $S + \gamma \rightarrow G + \gamma + \gamma$. The blue blobs represent the fermion Ψ loops.

II. MODEL

In this section, we start with the coloron model, which is gauged under $SU(3)_1 \times SU(3)_2$ spontaneously breaking down to QCD $SU(3)_C$ [83–85]. The spontaneous breaking is induced by a bi-triplet scalar Φ , a 3×3 matrix charged under $SU(3)_1 \times SU(3)_2$ as $(3, \bar{3})$ representation. Besides the gauge fields, heavy vector fermions and color-octet scalar and their interactions are considered here. The colored heavy particles are produced by and can decay to the Standard Model particles.

II.1. spontaneous breaking down to $SU(3)_C$

The Lagrangian for the kinetic term for G_1 , G_2 and scalar Φ are given as

$$\mathcal{L}^{\text{kin}} = -\frac{1}{4}G_{1,\mu\nu}^a G_1^{a,\mu\nu} - \frac{1}{4}G_{2,\mu\nu}^a G_2^{a,\mu\nu} + \text{Tr} \left[(D_\mu \Phi)^\dagger D^\mu \Phi \right], \quad (1)$$

where G_1 and G_2 are the field strength of $SU(3)_1$ and $SU(3)_2$ respectively. a is the color index running through 1 to 8. The covariant derivative of Φ field is,

$$D_\mu \Phi = \partial_\mu \Phi - ig_1 G_{1,\mu}^a T^a \Phi + ig_2 G_{2,\mu}^a T^a \Phi, \quad (2)$$

where $g_i (i = 1, 2)$ is the gauge coupling of the $SU(3)_i$ gauge group and $G_{i,\mu}$ is the corresponding gauge field for $SU(3)_i$. We use G_i for both gauge field strength and gauge field itself. When this notation is confusing, we add Lorentz indices $\mu\nu$ or μ to distinguish them.

We take the spontaneous breaking pattern of Φ to be $\langle \Phi \rangle = v_\Phi \mathbf{I} / \sqrt{6}$, where \mathbf{I} is the 3×3 identity matrix. We can read out the vector which gets mass after the spontaneous breaking from

$$\langle D_\mu \Phi \rangle \rightarrow i \left(-g_1 G_{1,\mu}^a + g_2 G_{2,\mu}^a \right) T^a \frac{v_\Phi}{\sqrt{6}}, \quad (3)$$

which shows that the linear combination $-g_1 G_{1,\mu}^a + g_2 G_{2,\mu}^a$ obtain mass and we denote it as G' . The other orthogonal combination remain massless and which is in fact the QCD gluon, denoted as G . The mixing matrices for G_1 and G_2 are given by

$$\begin{pmatrix} G_1 \\ G_2 \end{pmatrix} = \begin{pmatrix} \cos \theta_g & -\sin \theta_g \\ \sin \theta_g & \cos \theta_g \end{pmatrix} \begin{pmatrix} G' \\ G \end{pmatrix}, \quad (4)$$

where the mixing angle θ_g is defined by $\sin \theta_g \equiv -g_2 / \sqrt{g_1^2 + g_2^2}$ and $\cos \theta_g \equiv g_1 / \sqrt{g_1^2 + g_2^2}$. The mass of the colored vector G' is $m_{G'}^2 = (g_1^2 + g_2^2) v_\Phi^2 / 6$.

	SU(3) ₁	SU(3) ₂	SU(2) _L	U(1) _Y
G_1	8	1	1	0
G_2	1	8	1	0
Φ	3	$\bar{3}$	1	0
Ψ	3	1	1	Q_Y^Ψ
S	8	1	1	0
q_{SM}	1	3	Q_L^q	Q_Y^q

Table I. List of particle contents and their gauge charges. G_1 and G_2 are the vector gauge bosons for SU(3)₁ and SU(3)₂ respectively. Φ is a SU(3)₁ × SU(3)₂ bi-triplet, which is responsible for breaking SU(3)₁ × SU(3)₂ into SU(3)_C. Ψ is a heavy vector-like fermion and charged under SU(3)₁ and U(1)_Y. The SM quarks q_{SM} are charged under SU(3)₂, while the SU(2)_L and U(1)_Y charges are the same as that in SM which we do not explicitly write down. q_{SM} couples to octet G' through $G_{1,2}$ mixing, which is responsible for the resonance production of G' .

Considering the mixing between G' and G , we can get the strong coupling of the gluon self-interaction term

$$g_s \equiv g_1 g_2 / \sqrt{g_1^2 + g_2^2}. \quad (5)$$

The interactions between G' and gluon G are given as

$$\begin{aligned} \mathcal{L}_{G'G}^{\text{int}} = & \frac{1}{2} g_s^2 f^{abc} f^{ade} G'^{\mu b} \left\{ G^{\nu d} (G_\nu'^c G_\mu^e + G_\nu^c G_\mu'^e) + G_\nu'^e G^{\nu c} G_\mu^d \right\} \\ & + g_s f^{abc} G_\mu'^a \left\{ \left(\partial^\mu G'^{\nu b} - \partial^\nu G'^{\mu b} \right) G_\nu^c - G_\nu'^b \partial^\mu G^{\nu c} \right\}. \end{aligned} \quad (6)$$

We can see that in eq. (6), G' always appears as quadratic term. The reason is the kinetic term for G_1 and G_2 is symmetric under the operation $1 \leftrightarrow 2$. Under this operation, G' get a minus sign, while G does not change. Therefore, only quadratic G' appears in eq. (6). This prevent G' from decaying into gluons. After symmetry breaking, G' can be considered as a matter field charged under SU(3)_C. In G' kinetic term, there is no linear term in G' as well, for the same reason in eq. (6).

II.2. The interactions for extra fermions and scalars

We assign the SM quarks q_{SM} charged only under SU(3)₂ as fundamental representation. Their SU(2)_L and U(1)_Y charges are the same as that in SM, therefore we do not repeat them in the table. q_{SM} is coupled to octet G' through $G_{1,2}$ mixing, which is responsible for the resonance production of G' . Here we also introduce a SU(3)₁ octet scalar S without any other charge, and a heavy vector like fermion Ψ , charged only under SU(3)₁ as fundamental representation and also under hypercharge U(1)_Y. It has a dimension 5 operator $S^a G_{1,\mu\nu}^a B_{\mu\nu}$, which will induce the interactions for $S\gamma G'$ and $S\gamma G$. The mass of Ψ is assumed to be high to avoid G' and S decaying to Ψ pair. The summary of the gauge charges for the particles are listed in table I.

We list the relevant dimension 4 gauge interactions for fermions below

$$\begin{aligned} \mathcal{L}_{4d,F}^{\text{int}} = & -i g_1 G_{1,\mu}^a \bar{\Psi} \gamma^\mu T^a \Psi - i g_2 G_{2,\mu}^a \bar{q}_{\text{SM}} \gamma^\mu T^a q_{\text{SM}} \\ = & -i (g_1 \cos \theta_g G_\mu'^a + g_s G_\mu^a) \bar{\Psi} \gamma^\mu T^a \Psi - i (g_2 \sin \theta_g G_\mu'^a + g_s G_\mu^a) \bar{q}_{\text{SM}} \gamma^\mu T^a q_{\text{SM}}, \end{aligned} \quad (7)$$

where in the second line we expand $G_{1,2}$ into their mass eigenstates G' and G . For both Ψ and q_{SM} , the coupling to G is g_s due to they are fundamental representation of $\text{SU}(3)_C$. Since we assume Ψ is very heavy, the production of a Ψ pair through G is tiny. In our model, Ψ can be unstable and decay into SM particles to avoid cosmological limits¹.

The relevant dimension 4 operators for scalar S are given by

$$\mathcal{L}_{4d,S}^{\text{int}} \supset (D_\mu S)_a^\dagger (D_\mu S)_a + \lambda S^a \bar{\Psi} T^a \Psi, \quad (8)$$

$$(D_\mu S)_a = \alpha_\mu S_a - i g_1 f_{abc} G_{1,\mu}^b S^c = \alpha_\mu S_a - i f_{abc} \left(\cos \theta_g g_1 G_\mu'^b + g_s G_\mu^b \right) S^c, \quad (9)$$

where the color octet S is charged under $\text{SU}(3)_C$, which can be pair produced at the LHC. However, S does not couple to SM quarks, because they are assigned into different $\text{SU}(3)$ groups respectively and also due to the chirality of SM quarks.

II.3. The decay and production of G' and S

We are interested in the mass hierarchy where $m_\Psi, m_\Phi > m_{G'} > m_S$. How does G' and S decay in such hierarchy is important. The Yukawa term of S in eq. (8) can induce a dimension 5 operator,

$$\mathcal{L}_{5d}^{\text{int}} = k_S S^a G_{1,\mu\nu}^a B_{\mu\nu} = k_S S^a \left(\cos \theta_g G_{\mu\nu}'^a - \sin \theta_g G_{\mu\nu}^a \right) B_{\mu\nu}, \quad (10)$$

with

$$k_S = Q_Y^\Psi e \frac{\lambda g_1}{32\pi^2 m_\Psi} \tau (1 + (1 - \tau)f(\tau)), \quad (11)$$

where $\tau = 4m_\Psi^2/m_S^2$ and loop function [86, 87]

$$f(\tau) = \begin{cases} \arcsin^2(1/\sqrt{\tau}) & \text{for } \tau \geq 1 \\ \frac{1}{2} \left[\log \left(\frac{1+\sqrt{1-\tau}}{1-\sqrt{1-\tau}} \right) - i\pi \right]^2 & \text{for } \tau < 1 \end{cases}.$$

As Ψ is heavier than S , the loop factor $\tau (1 + (1 - \tau)f(\tau)) = 2/3$ in the limit of $\tau \rightarrow \infty$.

In our mass setup, S can only decay to $G + \gamma/Z$ via eq. (10). The corresponding decay widths of S are given by

$$\Gamma_{S \rightarrow G+\gamma} = (k_S \sin \theta_g \cos \theta_W)^2 \frac{m_S^3}{8\pi}, \quad (12)$$

$$\Gamma_{S \rightarrow G+Z} \approx (k_S \sin \theta_g \sin \theta_W)^2 \frac{m_S^3}{8\pi}. \quad (13)$$

Finally, the branching ratios of S decaying to $G\gamma$ and GZ equal to $\cos^2 \theta_W = 77\%$ and $\sin^2 \theta_W = 23\%$ respectively, where θ_W is the Weak angle as same in SM. Due to significant smaller branching ratio to Z and high sensitivity for γ detection, we will focus on the decay channel $S \rightarrow G + \gamma$. But for high luminosity 13 TeV data, the decay channel through Z is definitely worth exploring.

After mixing between G' and G , G' can decay to a pair of SM quarks. It also can decay to $S + \gamma/Z$ via loop operator in eq. (10). The formula of G' decay widths are given by

$$\Gamma_{G' \rightarrow \bar{q}q} = \frac{(g_2 \sin \theta_g)^2}{24\pi} m_{G'} \left(1 + 2 \frac{m_q^2}{m_{G'}^2} \right) \sqrt{1 - 4 \frac{m_q^2}{m_{G'}^2}}, \quad (14)$$

¹ If $Q_Y^\Psi = Q_Y^{u_R}$ where u_R is the SM right handed up quarks, Ψ can decay via Yukawa term $\bar{\Psi} \Phi u_R$. In eq. (1), after Φ obtain its vev, Φ can decay into two G' which is similar as SM Higgs decay to two Z boson. In more detail, the 3×3 matrix form of Φ can be written as $\Phi = \phi_0 I + \phi_8^a T^a$. eq. (1) contains operators like $\phi_0 G_\mu'^a G_\mu'^a$ and $d_{abc} \phi_8^a G_\mu'^b G_\mu'^c$, which can mediate the decay. Since G' can further decay to SM quarks, Ψ is unstable.

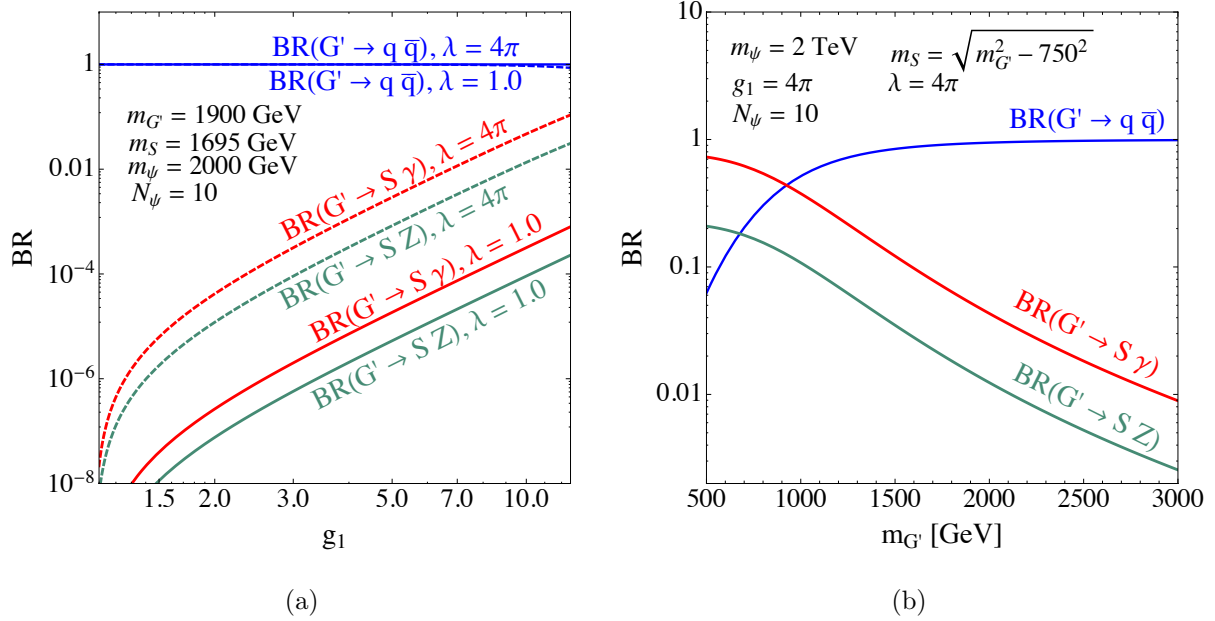


Figure 2. The G' decay branching ratio for $\bar{q}q$ (including all six flavor), $S + \gamma$ and $S + Z$ channels. N_Ψ is the copy of Ψ which has same hypercharge $Q_Y^\Psi = 1$. (a) the G' branching ratio as a function of g_1 . (b) the G' branching ratio as a function of $m_{G'}$.

$$\Gamma_{G' \rightarrow S + \gamma} = (k_S \cos \theta_g \cos \theta_W)^2 \frac{(m_{G'}^2 - m_S^2)^3}{24\pi m_{G'}^3}, \quad (15)$$

$$\Gamma_{G' \rightarrow S + Z} \approx (k_S \cos \theta_g \sin \theta_W)^2 \frac{(m_{G'}^2 - m_S^2)^3}{24\pi m_{G'}^3}. \quad (16)$$

We show the G' decay branching ratio in fig. 2. We generally need large $G' \rightarrow S + \gamma$ branching ratio to satisfy diphoton signal requirement and avoid collider constraints at the same time. Therefore, we assume a small mixing angle θ_g , which suggest that $g_1 \gg g_2$. This will suppress the decay width of $G' \rightarrow q\bar{q}$ by the coupling square $(g_2^2 / \sqrt{g_1^2 + g_2^2})^2$. To enhance the branching ratio of $G' \rightarrow S + \gamma$, we use $g_1 = 4\pi$, $\lambda = 4\pi$ and large N_Ψ copy of Ψ which has same hypercharge $Q_Y^\Psi = 1$.

In fig. 3, we show the single resonant production $\bar{q}q \rightarrow G'$ cross-section at 8(13) TeV as a function of $m_{G'}$. The calculation is done at tree level by MADGRAPH 5 v2.3 [88], with model implemented by FEYNRULES v2.3 [89]. We do not apply K-factor from QCD correction because it is only about 1.2 for $q\bar{q}$ production [8]. We also show cross-section for S pair production for constraint purpose.

III. CONSTRAINTS FOR THE MODEL

In our model, the resonance production of single G' will dominantly decay to SM quarks. This process will be constrained by the ATLAS 8 (13) TeV dijet invariant mass search [90, 91]. We choose their limits for W' hadronic decay and compare with our G' resonance cross-section, because they are both vector boson that the acceptance will be similar. For 8 (13) TeV, the dijet constraint shows that the cross-section times acceptance should be smaller than 60 (150) fb for W' at 2 TeV. We can see at this mass, our resonance cross-section of single G' is already smaller

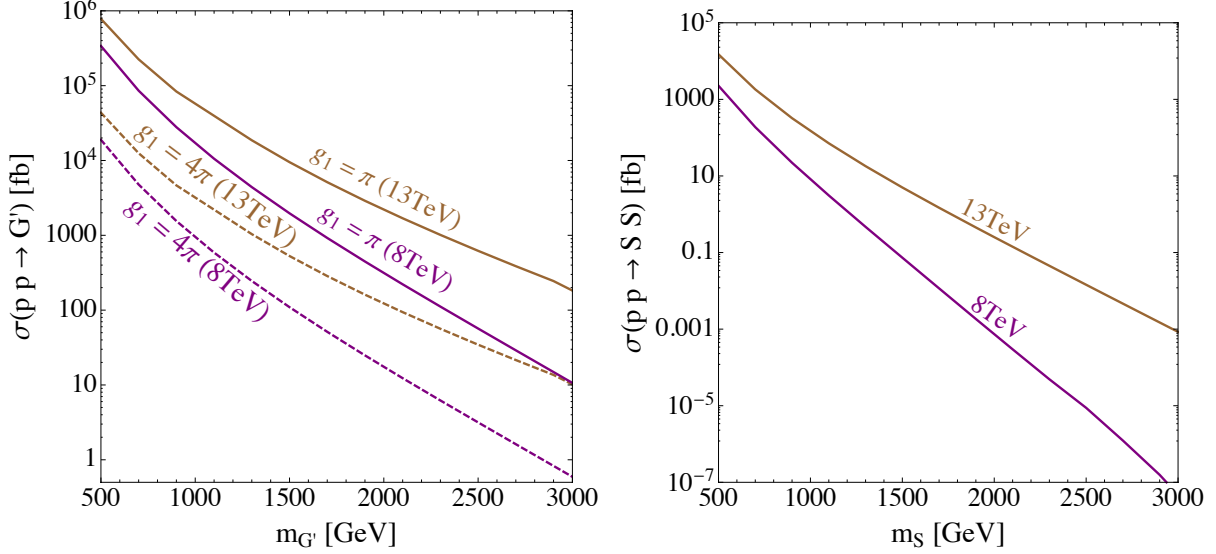


Figure 3. The single resonant production cross-section for $\bar{q}q \rightarrow G'$ and the pair production cross-section for $pp \rightarrow SS$. Note that the S pair production cross-section is only determined by strong interaction coupling g_s and m_S .

than the constraint. Including the acceptance will further weaken the constraints. Moreover, we should multiply by 5/6 from decay branching ratio of $G' \rightarrow \bar{q}q$, since it only constraints five flavor of quarks without top. If we conservatively assume that our signal acceptance is 1, we conclude that G' mass should be higher than 1450 (1250) GeV for 8 (13) TeV data.

The single resonance G' can also decay to $\bar{t}t$ whose branching ratio is 1/6 of the total branching ratio of $G' \rightarrow q\bar{q}$. ATLAS has searched for $\bar{t}t$ resonance through lepton-plus-jets topology at 8 TeV [92]. Their constraint for a resonant Z' which decay to $\bar{t}t$, is smaller than 50 fb at $m_{Z'} \sim 2$ TeV. This limit is comparable to dijet search. After considering the branching ratio of $G' \rightarrow \bar{t}t$, $\bar{t}t$ constraint is insensitive to the $G' \rightarrow \bar{t}t$ scenario.

Besides the constraints from G' , we should also consider the constraints from S , which decay to $G + \gamma$ with branching ratio around 77%. There are searches for jet-photon resonance from ATLAS at both 8 (13) TeV [93, 94]. The 95% CL limits on cross-section times acceptance are around 1 (10) fb at 8 (13) TeV respectively, for a jet+ γ resonance at 2 TeV. This search can place a stringent constraint for our model.

The S pair could be produced through gluon fusion $GG \rightarrow SS$ with strong coupling g_s , which is shown in eq. (8). The pair production cross-section is given in fig. 3. The S pair production cross-section decreases fast with increasing m_S , due to the two heavy S in the final states.

Therefore, we should also consider single productions of S , which might have larger cross-section. First there is no single production of S from G coupling as shown in eq. (8). However, it can be produced from cascade decay of G' and associate production with a photon via coupling $G - \gamma - S$.

For the cascade decay, it depends on the single production cross-section of G' and decay branching ratio $BR(G' \rightarrow S + \gamma)$. G' single production cross-section is determined by its quark coupling $g_2 \sin \theta_g$, where we choose $g_1 = 4\pi$ to fix the coupling due to the diphoton signal requirement. The decay branching ratio of $G' \rightarrow S + \gamma$ depends on masses and couplings.

For the associate production, we have calculated its cross-section using the same parameter in G' cascade by MADGRAPH 5 v2.3 [88]. We found that it is much smaller than G' cascade. By comparing the couplings and branching ratio formula, both of them are suppressed by the dimension

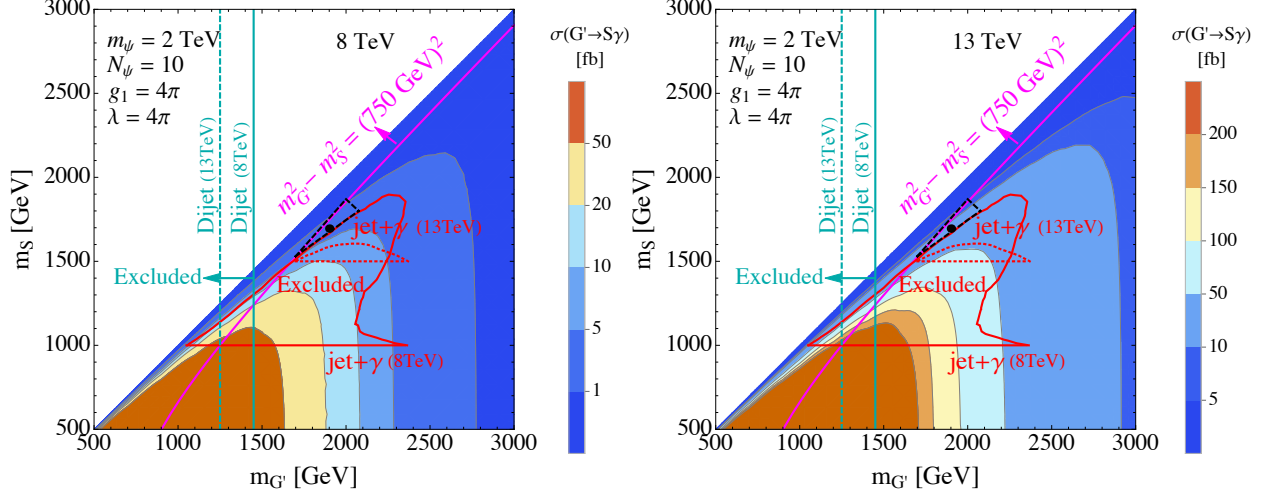


Figure 4. The cross-section for the process $\bar{q}q \rightarrow G' \rightarrow S + \gamma$ for 8 (13) TeV respectively. The constraints from dijet, jet+ γ resonance searches are shown for 8 (13) TeV respectively. The requirement from $m_{\gamma\gamma}$ edge in eq. (17) is shown as magenta line. The benchmark point is shown as a black dot. The best fit region for the signal is inside the black dashed triangle.

5 operator. However, the dimension 5 coupling for associate production is further suppressed by $\sin \theta_g$, see eq. (10). Furthermore, it is a 2 to 2 production, while G' cascade is a single resonant production. As a result, S associate production with photon does not provide constraints nor can it provide diphoton events to the signal.

In summary, the important production of S particles are pair production process $GG \rightarrow SS$ and cascade production $\bar{q}q \rightarrow G' \rightarrow S + \gamma$. We add the two cross-section together and conservatively assume that its acceptance in jet+ γ resonance search is 100%. In 8 (13) TeV data, we use the 95% CL limits from excited quark q^* . Note that the limits on the q^* mass stops at 1 (1.5) TeV for 8 (13) TeV data respectively. We show the constraints from jet+ γ resonance searches in fig. 4.

To summarize all the constraints, we put the dijet, jet+ γ resonance searches in fig. 4. The figure is the $m_{G'} - m_S$ 2D plot, with other parameters fixed for the signal. The cross-section for the process $\bar{q}q \rightarrow G' \rightarrow S + \gamma$ is given as color code in the plots, for 8 (13) TeV respectively. The dijets constraints require G' mass should be higher than 1450 (1250) GeV for 8 (13) TeV data respectively, and is shown as vertical solid(dashed) cyan lines. The jet+ γ constraints are shown as solid(dashed) red contours for 8 (13) TeV data respectively. The region inside the red contours are excluded. The regions where m_S is smaller than the horizontal red lines are not excluded, due to lack of data from experiments.

IV. DIPHOTON SIGNAL FROM CASCADE DECAY OF G'

In this section, we are going to explain the possible excess in the diphoton events, via resonant produced G' cascade decay. The decay chain is $G' \rightarrow S + \gamma \rightarrow G + \gamma + \gamma$, and the Feynman diagram is given in fig. 1.

Such decay chain has a well-known kinetic edge for the invariant mass of two photons $m_{\gamma\gamma}$ [95].

$$(m_{\gamma\gamma}^2)_{\max} = \frac{(m_{G'}^2 - m_S^2)(m_S^2 - m_G^2)}{m_S^2} = m_{G'}^2 - m_S^2 \quad (17)$$

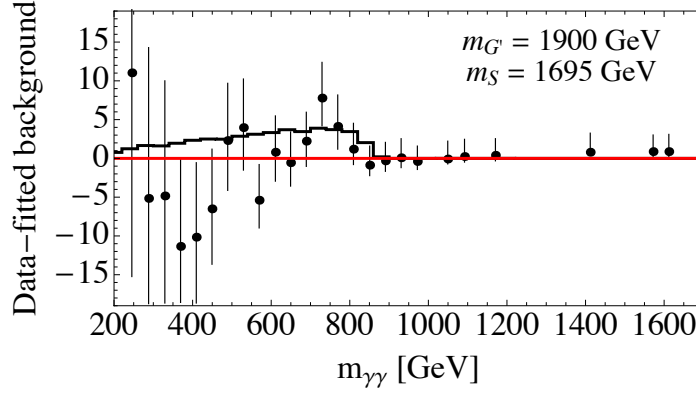


Figure 5. The $m_{\gamma\gamma}$ distribution for the benchmark point $\{m_{G'}, m_S\} = \{1900, 1695\}$ GeV. The data comes from ATLAS 13 TeV diphoton search [1]. The cross-section of the benchmark point is $\sigma(\bar{q}q \rightarrow G' \rightarrow S + \gamma) \times BR(S \rightarrow G + \gamma) = 14\text{fb}$, which determines the normalization of the signal.

We show our benchmark points $\{m_{G'}, m_S\} = \{1900, 1695\}$ GeV in fig. 4 and found it is consistent with all the dijet and jet+ γ resonance constraint. The parameter region which fits the diphoton signal for both shape and signal strength should have two requirements. First, it should be close to the $m_{G'}^2 - m_S^2 = (750\text{GeV})^2$ line, which is the requirement from $m_{\gamma\gamma}$ shape has the correct falling edge around 750 GeV. Second, it should have a cross-section for $\bar{q}q \rightarrow G' \rightarrow S + \gamma$ times $BR(S \rightarrow G + \gamma) = 77\%$ in the range about $\mathcal{O}(10)$ fb. This estimation is coming from the fact that for either short ($\Gamma_{\gamma\gamma} = 5$ GeV) or broad ($\Gamma_{\gamma\gamma} = 45$ GeV) diphoton resonance, the 2σ region for signal cross-section is between $[1, 11]$ fb [38]. Our fit to the signal is not resonance but kinetic edge, thus our signal cross-section should be larger. The estimated signal region is given inside the black dashed triangle in fig. 4. For the region above the $m_{G'}^2 - m_S^2 = (750\text{GeV})^2$ line, the $m_{\gamma\gamma}$ kinetic edge will move to smaller values.

Note that when we estimate the constraint, we conservatively assume signal acceptance equals to 100%. The actual limits might be weaker than our conservative limits, thus more parameter space opens up.

In fig. 5, we show the $m_{\gamma\gamma}$ distribution for the benchmark point $\{m_{G'}, m_S\} = \{1900, 1695\}$ GeV and compare with the ATLAS 13 TeV diphoton data. We see that the signal shape provide a right drop off around 750 GeV. In the small $m_{\gamma\gamma}$ region, our signal provides significant events there, which is one difference from the real diphoton resonance. We should remind that in fig. 5, the normalization of the signal is not arbitrary but fixed by the cross-section of signal: $\sigma(\bar{q}q \rightarrow G' \rightarrow S + \gamma) \times BR(S \rightarrow G + \gamma) = 14\text{fb}$.

Despite the different $m_{\gamma\gamma}$ shape, our signal also have other features. The normalized kinetic variable distribution for the benchmark point $\{m'_{G'}, m_S\} = \{1900, 1695\}$ GeV are shown in fig. 6. The left panel shows the p_T distribution for leading (γ_1), subleading (γ_2) photons and leading jet (j_1). We see that the subleading photon has p_T much smaller than leading jet, satisfying $p_T^{\gamma_2} < E^{\gamma_2} \sim (m_{G'}^2 - m_S^2)/(2m_{G'})$. G' is assumed to be produced at rest in the lab frame, which is a good estimation because it is very heavy. The leading photon and leading jet has quite large p_T , which are also the feature of our signal. Generally, in diphoton signal from gluon gluon fusion, the leading jet p_T will be much smaller than our signal.

The right panel shows the invariant mass distribution for the combination of $m_{\gamma_1\gamma_2}$, m_{j_1,γ_1} , $m_{j_1\gamma_2}$ and $m_{j_1\gamma_1\gamma_2}$. We can see quite easily that $m_{j_1\gamma_1\gamma_2}$ and m_{j_1,γ_1} distribution show the resonance from G' and S . $m_{\gamma_1\gamma_2}$ distribution drops around 750 GeV giving an non-resonant interpretation

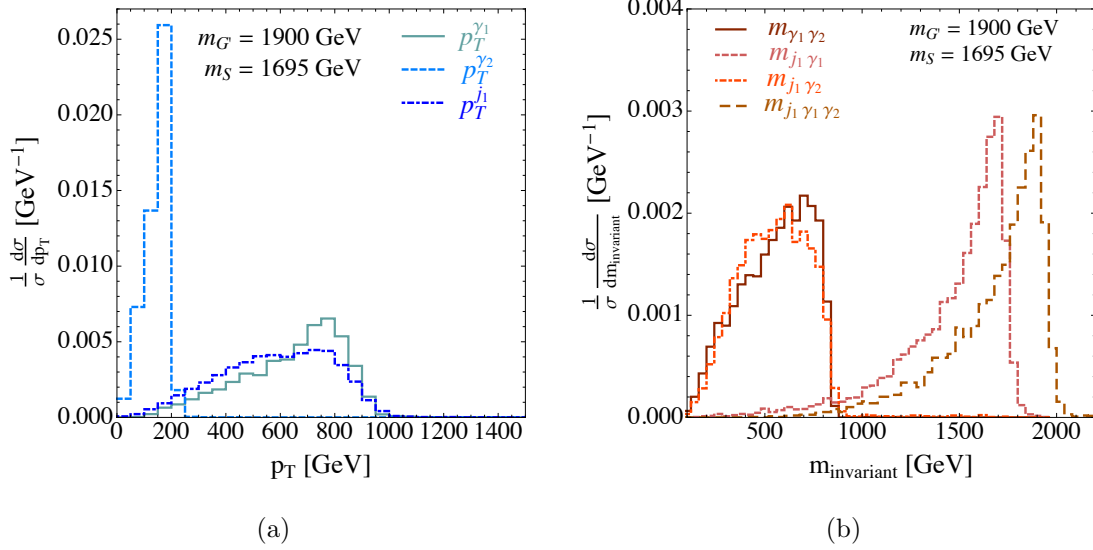


Figure 6. The normalized kinetic variable distribution for the benchmark point $\{m_{G'}, m_S\} = \{1900, 1695\}$ GeV. (a) the p_T distribution for leading (γ_1), subleading (γ_2) photons and leading jet (j_1). (b) the invariant mass distribution for the combination of $m_{\gamma_1 \gamma_2}$, $m_{j_1 \gamma_1}$, $m_{j_1 \gamma_2}$ and $m_{j_1 \gamma_1 \gamma_2}$.

to the possible diphoton excess. The $m_{j_1 \gamma_2}$ distribution follows $m_{\gamma_1 \gamma_2}$, because γ_1 is most likely coming from S decay that it has a similar momentum as j_1 .

In summary, given the above difference in p_T distribution and more invariant mass resonances, we can distinguish our signal from the other models which directly having a singlet 750 GeV particle decay to diphoton. We eagerly wait for more data to see if the diphoton excess is a statistic fluctuation or not, and check whether we can see more resonances in the events to validate our model.

V. SUMMARY AND CONCLUSION

In summary, we discuss that the cascade decay of a color octet vector G' at $\mathcal{O}(\text{TeV})$ can explain the 750 GeV diphoton excess at LHC 13 TeV. In the coloron model, we also introduce a color octet scalar S coupling to photon via heavy fermion Ψ loop, which leads to the cascade decay of G' . The final states are two photons and one gluon, where the invariant mass of the two photons has a kinetic edge around 750 GeV, resulting in the diphoton excess.

We start with the $\text{SU}(3)_1 \times \text{SU}(3)_2 \rightarrow \text{SU}(3)_C$ renormalizable model, which helps us understanding the relation between different couplings as discussed in section II. This setup reduces the number of free parameters and helps to find the right parameter region to interpret the diphoton excess. Generally, the resonance production of $q\bar{q} \rightarrow G'$ followed by cascade decay, faces the diphoton constraint from 8 TeV search. However in our case, the mass of G' is around TeV scale which is larger than 750 GeV, so that the quark luminosity function ratio can be quite large between 13 TeV and 8 TeV. Finally, we also check the collider constraints on this model, including resonance searches in dijet, $t\bar{t}$ and jet+ γ channels at both 8 (13) TeV as shown in fig. 4. Our benchmark point for the diphoton excess is safe under these constraints.

To conclude, the diphoton excess can be explained by the renormalizable coloron model, which has a number of unique features. First, all the new particles are charged under $\text{SU}(3)_C$, either triplet or octet. Secondly, unlike the diphoton decay from a scalar particle, we explain the diphoton excess

as the kinetic edge of cascade decay. Thirdly, we have two new resonances in the event. One is a jet+ γ resonance from octet scalar, and the other is jet+2 γ resonance from octet vector. Finally, the signal event usually contains a subleading photon with $p_T \lesssim 200$ GeV photon and a quite hard leading jet. With the above unique features, the model is quite easy to be tested with more data from LHC.

ACKNOWLEDGMENTS

We thank Michael J. Baker, Joachim Kopp, Ninetta Saviano, Yotam Soreq, Andrea Thamm, Jesse Thahler, Maikel de Vries, Felix Yu and Hua Xing Zhu for useful discussions. The work of JL is supported by the German Research Foundation (DFG) in the framework of the Research Unit “New Physics at the Large Hadron Collider” (FOR 2239) and of Grant No. KO 4820/1–1. The work of WX is support by the U.S. Department of Energy under grant Contract Numbers DE-SC00012567 and DE-SC0013999.

-
- [1] *Search for resonances decaying to photon pairs in 3.2 fb^{-1} of pp collisions at $\sqrt{s} = 13 \text{ TeV}$ with the ATLAS detector*, Tech. Rep. ATLAS-CONF-2015-081, CERN, Geneva, Dec, 2015.
 - [2] **CMS Collaboration Collaboration**, *Search for new physics in high mass diphoton events in proton-proton collisions at $\sqrt{s} = 13 \text{ TeV}$* , Tech. Rep. CMS-PAS-EXO-15-004, CERN, Geneva, 2015.
 - [3] Y. Mambrini, G. Arcadi, and A. Djouadi, *The Lhc Diphoton Resonance and Dark Matter*, 1512.04913.
 - [4] K. Harigaya and Y. Nomura, *Composite Models for the 750 GeV Diphoton Excess*, 1512.04850.
 - [5] M. Backovic, A. Mariotti, and D. Redigolo, *Di-Photon Excess Illuminates Dark Matter*, 1512.04917.
 - [6] Y. Nakai, R. Sato, and K. Tobioka, *Footprints of New Strong Dynamics via Anomaly*, 1512.04924.
 - [7] D. Buttazzo, A. Greljo, and D. Marzocca, *Knocking on New Physics’ Door with a Scalar Resonance*, 1512.04929.
 - [8] R. Franceschini, G. F. Giudice, J. F. Kamenik, M. McCullough, A. Pomarol, R. Rattazzi, M. Redi, F. Riva, A. Strumia, and R. Torre, *What is the gamma gamma resonance at 750 GeV?*, 1512.04933.
 - [9] S. Di Chiara, L. Marzola, and M. Raidal, *First Interpretation of the 750 GeV Di-Photon Resonance at the Lhc*, 1512.04939.
 - [10] A. Angelescu, A. Djouadi, and G. Moreau, *Scenarii for interpretations of the LHC diphoton excess: two Higgs doublets and vector-like quarks and leptons*, 1512.04921.
 - [11] S. Knapen, T. Melia, M. Papucci, and K. Zurek, *Rays of Light from the Lhc*, 1512.04928.
 - [12] A. Pilaftsis, *Diphoton Signatures from Heavy Axion Decays at Lhc*, 1512.04931.
 - [13] J. Ellis, S. A. R. Ellis, J. Quevillon, V. Sanz, and T. You, *On the Interpretation of a Possible $\sim 750 \text{ GeV}$ Particle Decaying into $\gamma\gamma$* , 1512.05327.
 - [14] B. Bellazzini, R. Franceschini, F. Sala, and J. Serra, *Goldstones in Diphotons*, 1512.05330.
 - [15] R. S. Gupta, S. Jäger, Y. Kats, G. Perez, and E. Stamou, *Interpreting a 750 GeV Diphoton Resonance*, 1512.05332.
 - [16] E. Molinaro, F. Sannino, and N. Vignaroli, *Minimal Composite Dynamics Versus Axion Origin of the Diphoton Excess*, 1512.05334.
 - [17] T. Higaki, K. S. Jeong, N. Kitajima, and F. Takahashi, *The QCD Axion from Aligned Axions and Diphoton Excess*, 1512.05295.
 - [18] S. D. McDermott, P. Meade, and H. Ramani, *Singlet Scalar Resonances and the Diphoton Excess*, 1512.05326.
 - [19] M. Low, A. Tesi, and L.-T. Wang, *A Pseudoscalar Decaying to Photon Pairs in the Early Lhc Run 2 Data*, 1512.05328.
 - [20] C. Petersson and R. Torre, *The 750 GeV Diphoton Excess from the Goldstino Superpartner*, 1512.05333.

- [21] B. Dutta, Y. Gao, T. Ghosh, I. Gogoladze, and T. Li, *Interpretation of the Diphoton Excess at Cms and Atlas*, 1512.05439.
- [22] Q.-H. Cao, Y. Liu, K.-P. Xie, B. Yan, and D.-M. Zhang, *A Boost Test of Anomalous Diphoton Resonance at the Lhc*, 1512.05542.
- [23] S. Matsuzaki and K. Yamawaki, *750 GeV Diphoton Signal from One-Family Walking Technipion*, 1512.05564.
- [24] A. Kobakhidze, F. Wang, L. Wu, J. M. Yang, and M. Zhang, *Lhc 750 GeV Diphoton Resonance Explained as a Heavy Scalar in Top-Seesaw Model*, 1512.05585.
- [25] P. Cox, A. D. Medina, T. S. Ray, and A. Spray, *Diphoton Excess at 750 GeV from a Radion in the Bulk-Higgs Scenario*, 1512.05618.
- [26] A. Ahmed, B. M. Dillon, B. Grzadkowski, J. F. Gunion, and Y. Jiang, *Higgs-Radion Interpretation of 750 GeV Di-Photon Excess at the Lhc*, 1512.05771.
- [27] P. Agrawal, J. Fan, B. Heidenreich, M. Reece, and M. Strassler, *Experimental Considerations Motivated by the Diphoton Excess at the Lhc*, 1512.05775.
- [28] R. Martínez, F. Ochoa, and C. F. Sierra, *Diphoton Decay for a 750 GeV Scalar Boson in an $U(1)'$ Model*, 1512.05617.
- [29] D. Becirevic, E. Bertuzzo, O. Sumensari, and R. Z. Funchal, *Can the New Resonance at Lhc Be a Cp -Odd Higgs Boson?*, 1512.05623.
- [30] J. M. No, V. Sanz, and J. Setford, *See-Saw Composite Higgses at the Lhc: Linking Naturalness to the 750 GeV Di-Photon Resonance*, 1512.05700.
- [31] S. V. Demidov and D. S. Gorbunov, *On Sgoldstino Interpretation of the Diphoton Excess*, 1512.05723.
- [32] W. Chao, R. Huo, and J.-H. Yu, *The Minimal Scalar-Stealth Top Interpretation of the Diphoton Excess*, 1512.05738.
- [33] S. Fichtel, G. von Gersdorff, and C. Royon, *Scattering Light by Light at 750 GeV at the LHC*, 1512.05751.
- [34] D. Curtin and C. B. Verhaaren, *Quirky Explanations for the Diphoton Excess*, 1512.05753.
- [35] L. Bian, N. Chen, D. Liu, and J. Shu, *A Hidden Confining World on the 750 GeV Diphoton Excess*, 1512.05759.
- [36] J. Chakraborty, A. Choudhury, P. Ghosh, S. Mondal, and T. Srivastava, *Di-Photon Resonance Around 750 GeV: Shedding Light on the Theory Underneath*, 1512.05767.
- [37] C. Csaki, J. Hubisz, and J. Terning, *The Minimal Model of a Diphoton Resonance: Production without Gluon Couplings*, 1512.05776.
- [38] A. Falkowski, O. Slone, and T. Volansky, *Phenomenology of a 750 GeV Singlet*, 1512.05777.
- [39] D. Aloni, K. Blum, A. Dery, A. Efrati, and Y. Nir, *On a Possible Large Width 750 GeV Diphoton Resonance at Atlas and Cms*, 1512.05778.
- [40] Y. Bai, J. Berger, and R. Lu, *A 750 GeV Dark Pion: Cousin of a Dark G -Parity-Odd WIMP*, 1512.05779.
- [41] E. Gabrielli, K. Kannike, B. Mele, M. Raidal, C. Spethmann, and H. Veermäe, *A SUSY Inspired Simplified Model for the 750 GeV Diphoton Excess*, 1512.05961.
- [42] R. Benbrik, C.-H. Chen, and T. Nomura, *Higgs Singlet as a Diphoton Resonance in a Vector-Like Quark Model*, 1512.06028.
- [43] J. S. Kim, J. Reuter, K. Rolbiecki, and R. R. de Austri, *A Resonance without Resonance: Scrutinizing the Diphoton Excess at 750 GeV*, 1512.06083.
- [44] A. Alves, A. G. Dias, and K. Sinha, *The 750 GeV S -cion: Where Else Should We Look for It?*, 1512.06091.
- [45] E. Megias, O. Pujolas, and M. Quiros, *On Dilatons and the Lhc Diphoton Excess*, 1512.06106.
- [46] L. M. Carpenter, R. Colburn, and J. Goodman, *Supersoft SUSY Models and the 750 GeV Diphoton Excess, Beyond Effective Operators*, 1512.06107.
- [47] J. Bernon and C. Smith, *Could the width of the diphoton anomaly signal a three-body decay ?*, 1512.06113.
- [48] O. Antipin, M. Mojaza, and F. Sannino, *A Natural Coleman-Weinberg Theory Explains the Diphoton Excess*, 1512.06708.
- [49] F. Wang, L. Wu, J. M. Yang, and M. Zhang, *750 GeV Diphoton Resonance, 125 GeV Higgs and Muon $G-2$ Anomaly in Deflected Anomaly Mediation SUSY Breaking Scenario*, 1512.06715.

- [50] J. Cao, C. Han, L. Shang, W. Su, J. M. Yang, and Y. Zhang, *Interpreting the 750 GeV Diphoton Excess by the Singlet Extension of the Manohar-Wise Model*, 1512.06728.
- [51] F. P. Huang, C. S. Li, Z. L. Liu, and Y. Wang, *750 GeV Diphoton Excess from Cascade Decay*, 1512.06732.
- [52] W. Liao and H.-q. Zheng, *Scalar Resonance at 750 GeV as Composite of Heavy Vector-Like Fermions*, 1512.06741.
- [53] J. J. Heckman, *750 GeV Diphotons from a D3-Brane*, 1512.06773.
- [54] M. Dhuria and G. Goswami, *Perturbativity, Vacuum Stability and Inflation in the Light of 750 GeV Diphoton Excess*, 1512.06782.
- [55] X.-J. Bi, Q.-F. Xiang, P.-F. Yin, and Z.-H. Yu, *The 750 GeV Diphoton Excess at the Lhc and Dark Matter Constraints*, 1512.06787.
- [56] J. S. Kim, K. Rolbiecki, and R. R. de Austri, *Model-Independent Combination of Diphoton Constraints at 750 GeV*, 1512.06797.
- [57] L. Berthier, J. M. Cline, W. Shepherd, and M. Trott, *Effective Interpretations of a Diphoton Excess*, 1512.06799.
- [58] W. S. Cho, D. Kim, K. Kong, S. H. Lim, K. T. Matchev, J.-C. Park, and M. Park, *The 750 GeV Diphoton Excess May Not Imply a 750 GeV Resonance*, 1512.06824.
- [59] J. M. Cline and Z. Liu, *Lhc Diphotons from Electroweakly Pair-Produced Composite Pseudoscalars*, 1512.06827.
- [60] M. Bauer and M. Neubert, *Flavor Anomalies, the Diphoton Excess and a Dark Matter Candidate*, 1512.06828.
- [61] M. Chala, M. Duerr, F. Kahlhoefer, and K. Schmidt-Hoberg, *Tricking Landau-Yang: How to Obtain the Diphoton Excess from a Vector Resonance*, 1512.06833.
- [62] K. Kulkarni, *Extension of ν MSM Model and Possible Explanations of Recent Astronomical and Collider Observations*, 1512.06836.
- [63] D. Barducci, A. Goudelis, S. Kulkarni, and D. Sengupta, *One Jet to Rule Them All: Monojet Constraints and Invisible Decays of a 750 GeV Diphoton Resonance*, 1512.06842.
- [64] S. M. Boucenna, S. Morisi, and A. Vicente, *The Lhc Diphoton Resonance from Gauge Symmetry*, 1512.06878.
- [65] C. W. Murphy, *Vector Leptoquarks and the 750 GeV Diphoton Resonance at the Lhc*, 1512.06976.
- [66] A. E. C. Hernández and I. Nisandzic, *LHC diphoton 750 GeV resonance as an indication of $SU(3)_c \times SU(3)_L \times U(1)_X$ gauge symmetry*, 1512.07165.
- [67] U. K. Dey, S. Mohanty, and G. Tomar, *750 GeV Resonance in the Dark Left-Right Model*, 1512.07212.
- [68] G. M. Pelaggi, A. Strumia, and E. Vigiani, *Trinification Can Explain the Di-Photon and Di-Boson Lhc Anomalies*, 1512.07225.
- [69] J. de Blas, J. Santiago, and R. Vega-Morales, *New Vector Bosons and the Diphoton Excess*, 1512.07229.
- [70] A. Belyaev, G. Cacciapaglia, H. Cai, T. Flacke, A. Parolini, and H. Serôdio, *Singlets in Composite Higgs Models in light of the LHC di-photon searches*, 1512.07242.
- [71] P. S. B. Dev and D. Teresi, *Asymmetric Dark Matter in the Sun and the Diphoton Excess at the Lhc*, 1512.07243.
- [72] W.-C. Huang, Y.-L. S. Tsai, and T.-C. Yuan, *Gauged Two Higgs Doublet Model confronts the LHC 750 GeV di-photon anomaly*, 1512.07268.
- [73] S. Moretti and K. Yagyu, *The 750 GeV diphoton excess and its explanation in 2-Higgs Doublet Models with a real inert scalar multiplet*, 1512.07462.
- [74] K. M. Patel and P. Sharma, *Interpreting 750 GeV diphoton excess in $SU(5)$ grand unified theory*, 1512.07468.
- [75] M. Badziak, *Interpreting the 750 GeV diphoton excess in minimal extensions of Two-Higgs-Doublet models*, 1512.07497.
- [76] S. Chakraborty, A. Chakraborty, and S. Raychaudhuri, *Diphoton resonance at 750 GeV in the broken MRSSM*, 1512.07527.
- [77] Q.-H. Cao, S.-L. Chen, and P.-H. Gu, *Strong CP Problem, Neutrino Masses and the 750 GeV Diphoton Resonance*, 1512.07541.

- [78] W. Altmannshofer, J. Galloway, S. Gori, A. L. Kagan, A. Martin, and J. Zupan, *On the 750 GeV di-photon excess*, 1512.07616.
- [79] M. Cvetič, J. Halverson, and P. Langacker, *String Consistency, Heavy Exotics, and the 750 GeV Diphoton Excess at the LHC*, 1512.07622.
- [80] J. Gu and Z. Liu, *Running after Diphoton*, 1512.07624.
- [81] C.-N. Yang, *Selection Rules for the Dematerialization of a Particle Into Two Photons*, *Phys. Rev.* **77** (1950) 242–245.
- [82] *65-on the angular momentum of a system of two photons*, in *Collected Papers of L.D. Landau* (D. T. HAAR, ed.), pp. 471 – 473. Pergamon, 1965.
- [83] P. H. Frampton and S. L. Glashow, *Chiral Color: An Alternative to the Standard Model*, *Phys. Lett.* **B190** (1987) 157.
- [84] J. Bagger, C. Schmidt, and S. King, *AXIGLUON PRODUCTION IN HADRONIC COLLISIONS*, *Phys.Rev.* **D37** (1988) 1188.
- [85] C. T. Hill and E. H. Simmons, *Strong dynamics and electroweak symmetry breaking*, *Phys. Rept.* **381** (2003) 235–402, [[hep-ph/0203079](#)]. [Erratum: *Phys. Rept.*390,553(2004)].
- [86] J. R. Ellis, M. K. Gaillard, and D. V. Nanopoulos, *A Phenomenological Profile of the Higgs Boson*, *Nucl. Phys.* **B106** (1976) 292.
- [87] M. A. Shifman, A. I. Vainshtein, M. B. Voloshin, and V. I. Zakharov, *Low-Energy Theorems for Higgs Boson Couplings to Photons*, *Sov. J. Nucl. Phys.* **30** (1979) 711–716. [*Yad. Fiz.*30,1368(1979)].
- [88] J. Alwall, R. Frederix, S. Frixione, V. Hirschi, F. Maltoni, O. Mattelaer, H. S. Shao, T. Stelzer, P. Torrielli, and M. Zaro, *The automated computation of tree-level and next-to-leading order differential cross sections, and their matching to parton shower simulations*, *JHEP* **07** (2014) 079, [[1405.0301](#)].
- [89] A. Alloul, N. D. Christensen, C. Degrande, C. Duhr, and B. Fuks, *FeynRules 2.0 - A complete toolbox for tree-level phenomenology*, *Comput. Phys. Commun.* **185** (2014) 2250–2300, [[1310.1921](#)].
- [90] **ATLAS Collaboration**, G. Aad *et al.*, *Search for new phenomena in the dijet mass distribution using $p - p$ collision data at $\sqrt{s} = 8$ TeV with the ATLAS detector*, *Phys. Rev.* **D91** (2015), no. 5 052007, [[1407.1376](#)].
- [91] **ATLAS Collaboration**, *Search for New Phenomena in Dijet Mass and Angular Distributions from pp Collisions at $\sqrt{s} = 13$ TeV with the ATLAS Detector*, 1512.01530.
- [92] **ATLAS Collaboration**, G. Aad *et al.*, *A search for $t\bar{t}$ resonances using lepton-plus-jets events in proton-proton collisions at $\sqrt{s} = 8$ TeV with the ATLAS detector*, *JHEP* **08** (2015) 148, [[1505.07018](#)].
- [93] **ATLAS Collaboration**, G. Aad *et al.*, *Search for new phenomena in photon+jet events collected in proton-proton collisions at $\sqrt{s} = 8$ TeV with the ATLAS detector*, *Phys. Lett.* **B728** (2014) 562–578, [[1309.3230](#)].
- [94] **ATLAS Collaboration**, G. Aad *et al.*, *Search for new phenomena with photon+jet events in proton-proton collisions at $\sqrt{s} = 13$ TeV with the ATLAS detector*, 1512.05910.
- [95] D. J. Miller, P. Osland, and A. R. Raklev, *Invariant mass distributions in cascade decays*, *JHEP* **03** (2006) 034, [[hep-ph/0510356](#)].